USBL POSITIONING SYSTEM: IMPLEMENTATION AND TESTS AT SEA

J. Picão, M. Morgado, P. Oliveira, C. Silvestre [1]

IST - Instituto Superior Técnico
ISR - Institute for Systems and Robotics
Av. Rovisco Pais, 1, 1049-001, Lisbon, Portugal
jnpicao@hotmail.com,
{marcomorgado,pjcro,cjs}@isr.ist.utl.pt

Abstract: This paper presents the design, implementation, and validation at sea of an Ultra Short Base Line (USBL) acoustic positioning system. Signal detection and TOA estimation are based on the matched filters of Direct Spread Spectrum Signal (DSSS) coded signals which allows for improved detection in a variety of SNR scenarios, and stronger multi-path rejection. Experimental validation tests were conducted inside an harbor, using both static and moving scenarios. Several Time Of Arrival (TOA) estimation techniques are tested, revealing excellent multi-path rejection rates and improved accuracy.

Keywords: USBL, Underwater Acoustic Positioning

1. INTRODUCTION

Among several available underwater navigation aiding sensors such as Doppler Velocity Loggers (DVL), depth pressure sensors, and magnetic compasses, acoustic positioning systems (see (Milne, 1983), and (Vickery, 1998)) like Long Base Line (LBL), Short Base Line (SBL), and Ultra-Short Base Line (USBL) stand often as the primary choice for underwater positioning (see (Lurton and Millard, 1994), (Smith and Kronen, 1997), (Larsen, 2000), and (Lee *et al.*, 2004)).

The USBL sensor consists of a small and compact array of acoustic transducers that allows for the computation of a transponder position in the vehicle coordinate frame, based on the travel time of acoustic signals emitted by the transponder. The measurements provided by these systems have very low update rates (typically below 1 Hz) imposed by physical limitations and mission specific constraints (velocity of acoustic waves in the water, multi-path phenomena, and other disturbances), with a performance that degrades as the transponder/USBL distance increases.

The opacity (i.e. high attenuation) of the ocean environment to most electromagnetic signals makes acoustic propagation the preferable method to obtain practical range measurements. Acoustic signals have been used for precise underwater range measurement by time-of-flight of acoustic waves in the last decades (Milne, 1983). Historically, due to the simplicity of the hardware involved, sinusoidal pulses were the primordial choice for underwater range measurements. Recent advances and the availability of low-cost, high-speed Digital Signal Processors (DSP) hardware and software, amplifiers and wide band acoustic transducers allow for the use of more advanced signaling techniques like CHIRP tone bursts and spread-spectrum signals (Austin, 1994; Bingham *et al.*, 2007). In general, spread-spectrum signals have several advantages when compared to conventional signaling for underwater range estimation: they present better Signal-to-Noise-Ratio (SNR), robustness to ambient and jamming noise, multi-user capabilities, improved detection jitter, and the ability to better resolve multi-path which is one of the biggest problems in underwater channel acoustic propagation.

[1] This work was supported by FCT (ISR/IST plurianual funding) through the PIDDAC Program funds, and partially funded by EU Project TRIDENT (Contract No. 248497). The work of M. Morgado was funded with grant SFRH/BD/25368/2005, from Fundação para a Ciência e a Tecnologia.

For any coherent detection problem, a good estimate of the Time-Of-Arrival (TOA) of a signal may be obtained by passing the input signal through a matched-filter whose impulse response is a time-reversed replica of the expected signal. In ideal conditions, the filter output is related to the autocorrelation function of the received signal. Specially designed spread-spectrum modulated signals have known good autocorrelation properties (Sarwate and Pursley, 1980) allowing for a sharper output of the matched-filter and improving the performance of the detector. Moreover, good cross-correlation properties can be obtained between several spread-spectrum signals allowing for a multi-user configuration in which several entities might be transmitting signals at the same time without interference. This specially designed signals are typically generated using either Frequency Hopped Spread Spectrum (FHSS) or Direct Sequence Spread Spectrum (DSSS) codes. In the scope of this work, we focus our attention on DSSS modulated signals and its performance as an acoustic ranging signal. Closely related work can be found in (Austin, 1994), (Bingham *et al.*, 2007), and in (Bingham *et al.*, 2005).

The paper is divided as follows: the USBL positioning scheme is detailed in Section 2. Section 3 provides some details on the prototype system hardware and software development, and Section 4 presents the experimental results from the sea trials and its analysis. Finally some concluding remarks and comments on future work are presented in Section 5.

2. USBL POSITIONING

The USBL positioning system computes the range and direction of the transponder resorting to the planar approximation of the acoustic waves as in the classical approach presented in (Yli-Hietanen *et al.*, 1996), and already used by the authors in (Morgado *et al.*, 2006). The positioning framework is illustrated in fig. 1 with two receivers (i and k) projected on XY plan, a propagating planar wave, time of arrival of the signal at the receivers (t_i and t_k) and the unit direction vector of the transponder $\mathbf{d} = \left[\, d_x \; d_y \; d_z \,\right]^T$.

Taking into account the planar wave approximation, it can be written that the TDOA between receivers i and k is given by

$$\delta^{(i,k)} = t_i - t_k = -\frac{1}{v_p}\mathbf{d}^T \left({}^B\mathbf{p}_{r_i} - {}^B\mathbf{p}_{r_k} \right) \quad (1)$$

where v_p is the speed of sound in the water, ${}^B\mathbf{p}_{r_g}$ is receiver g ($g = \{i,k\}$) position on Body frame and $\mathbf{d}$ is the unit direction vector of transponder j ($\|\mathbf{d}\|_2 = 1$).

The vector of TDOA between all possible combinations of N receivers is described, from (1) $\{i = 1,\ldots,N; k = 1,\ldots,N; i \neq k\}$, by

$$\mathbf{\Delta} = \left[\, {\delta^{(1,2)}}_1 \; {\delta^{(1,3)}}_2 \; \cdots \; {\delta^{(N-1,N)}}_M \,\right]^T$$

and it can be generated by

$$\mathbf{\Delta} = \mathbf{C}\mathbf{t}_m$$

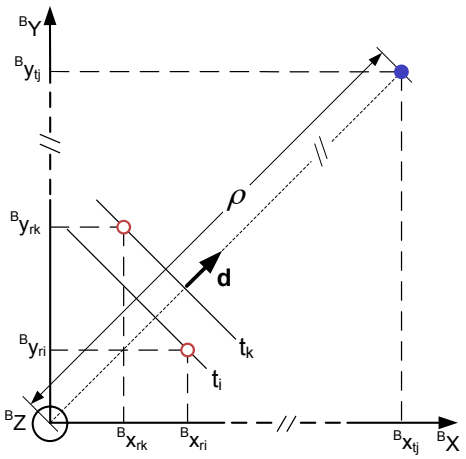

Fig. 1. Planar wave approximation

where $\mathbf{C}$ is a combination matrix and $\mathbf{t}_m$ is the vector of time measurements from all receivers given by

$$\mathbf{t}_m = \left[\, t_{1_m} \; t_{2_m} \; \cdots \; t_{N_m} \,\right]^T$$

Thus, the least squares solution for the transponder's j direction $\mathbf{d}$ is

$$\widehat{\mathbf{d}} = -v_p S^{\#} \mathbf{C}\mathbf{t}_m$$

where

$$S = \begin{bmatrix} x_1 - x_2 & y_1 - y_2 & z_1 - z_2 \\ x_1 - x_3 & y_1 - y_3 & z_1 - z_3 \\ \vdots & \vdots & \vdots \\ x_{N-1} - x_N & y_{N-1} - y_N & z_{N-1} - z_N \end{bmatrix}$$

and

$$S^{\#} = \left(S^T S\right)^{-1} S^T$$

Also resorting to the planar wave approximation, the range of transponder j to the origin of Body frame can be computed by averaging the range estimates from all receivers. The estimate for receiver h ($h = \{1,\ldots,N\}$) is given by

$$\widehat{\rho}_h = v_p t_h + {}^B\overline{\mathbf{p}}_{r_h}^T \mathbf{d} \quad (2)$$

Thus, averaging (2) for all N receivers yields

$$\widehat{\rho} = \frac{1}{N}\sum_{h=1}^{N} \left(v_p t_h + {}^B\overline{\mathbf{p}}_{r_h}^T \mathbf{d} \right)$$

3. EXPERIMENTAL SYSTEM DEVELOPMENT

In this section the design and development of the USBL acoustic positioning system is addressed with focus on data acquisition and signal processing. The proposed architecture consists mainly of two major standalone systems: the first is an emission system that is able to generate DSSS acoustic signals stored in memory. The latter is the reception system that is an ensemble between the acoustic array and all the workhorse that provides power, signal acquisition and processing. Both systems are synchronized with the 1PPS clock signal from GPS enabling the ability to

calibrate the underwater sound speed and evaluate the repeatability of the system.

The reception system electronics are housed inside a rectangular splash-proof case with four hydrophone input connectors, a GPS antenna for PPS signal access, an external power supply and an Ethernet port. The array is composed of 4 hydrophones placed in a non-planar configuration (that allows for 3D transponder localization) and is placed underwater using the structure depicted in Fig. 3

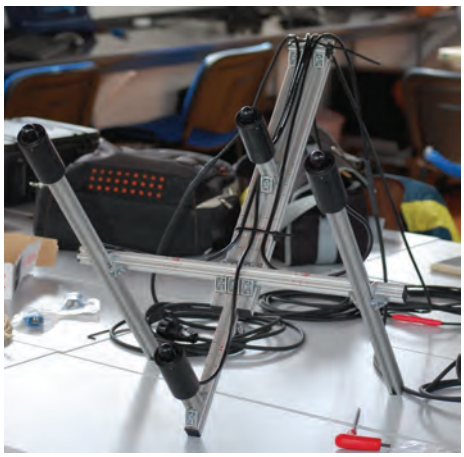

Fig. 2. USBL array structure

At the core of the reception box is the DSP that allows improved performance and versatility for the USBL acoustic positioning system. A C6713 floating-point DSP from Texas Instruments that operates at 300MHz was used, coupled to a 16 bit, 250 KSPS, 4 synchronous channel A/D converter and 4 variable gain amplifiers. The system is controlled (start/stop, operation mode, data transfer, ...) by a host PC and the communication is ensured by a DSign.T 91C111 Ethernet board.

To tackle the digital data storage problem, a FIFO (First-In-First-Out) data buffer was implemented. The buffer is divided into blocks and while the ADC is acquiring new data, the latest block of data available in the buffer is being processed. When the acquisition is completed the oldest block is replaced by the newest data and a new acquisition cycle begins. The number and length of the blocks is a major implementation criteria and a delicate problem because during the time of one block acquisition, given by L/f_s where L is the block length and f_s the sampling frequency, the DSP must be able to process the data present in all blocks of the buffer. Based on this time demand, the blocks must be large enough to allow for the data buffer processing but not too large due to memory constrains. This trade-off led to the use of blocks of the same length L as the expected signal.

A sketch of the buffer hardware implementation is shown in Fig. 3 as well as the progress of an expected signal through the buffer. As the system has four hydrophones there will be four FIFO buffers for data storage.

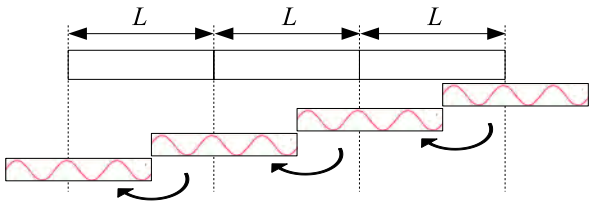

Fig. 3. FIFO data buffer of length $3L$

When the system indicates the presence of the expected signal, the signal may be completely or just partially inside the buffer. Thus, in order to obtain accurate results, before estimating the received signal TOA to the different hydrophones and compute emitter position, it must be ensured that the expected signal is completely inside the buffer. The option of using three blocks of length L is selected to ensure that the detection is performed twice, and ensuring that the second time the signal is detected, the signal is completely inside the data buffer and not partially. Thus, the first detection is always ignored and just the second consecutive detection is accepted when is guaranteed that the signal is completely inside the buffer. At this point the acquisition is temporarily stopped to allow for TOA estimation and the emitter's position computation, while adding robustness to multi-path. It is important to remark that if just two blocks of length L were used, it could not be guaranteed that the signal was not only partially inside the buffer on the first and/or second detection.

Exploiting the well known properties and equivalence between the convolution and the Discrete Fourier Transform (DFT), the matched-filters are implemented using Fast Fourier Transform (FFT) algorithms. Also, using the overlapping properties of the individual data buffer blocks when performing linear convolution it is possible to execute only one block convolution at each new acquisition cycle, implementing a commonly used algorithm known as Overlap-Add.

The decision criteria of whether a signal is present or not in the data buffer is motivated by the known good properties of the DSSS modulated signals and the basic idea behind the selected detectability criteria is to compare the maximum value of the matched filters output with its average absolute value. Thus, a suitable criteria for now is based on a threshold decision defined by

$$\frac{max\left\{y[n]\right\}}{avg\left\{|y[n]|\right\}} > threshold. \tag{3}$$

where $y[n]$ is the output of the matched-filter.

4. TRIALS AT SEA

To evaluate the performance of the system, a set of sea trials were conducted in Cidade da Horta, Azores, between June 22 and 26, 2009. The tests were divided into two main categories: stationary, in which both

the receiving array and the emitter are static - and dynamic, in which the emitter was moving aboard a small rubber boat while transmitting the DSSS signals synchronized with the 1PPS clock signal from GPS. Several boats were floating inside the marina besides the floating piers, and combined with a maximum depth of 9 meters, the test conditions were not ideal, in fact rather harsh and quite far from ideal. We feel that the results obtained are even strengthened by this fact.

4.1 *Stationary tests*

For the stationary tests the emitter was tied to a pier that suffers negligible fluctuations for the purpose intended and the system was left running for 20 minutes. The histogram of stationary distance results, as obtained during the test by DSP processing, is presented in Fig. 4.

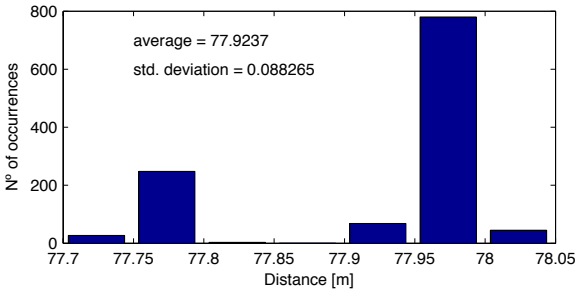

Fig. 4. Histogram of stationay test distance results

From Fig. 4 it can be seen that distance results are mostly divided between two non-contiguous sub-intervals, $[77.70; 77.80]m$ and $[77.90; 78.05]m$. Being the emitter and the USBL array both stationary it was an unexpected result. This first preliminary results let to a deeper analysis of the receiving signals in order to fully understand the unexpected unbalance. The output of the matched filter for two different detections is shown in Figs. 5.

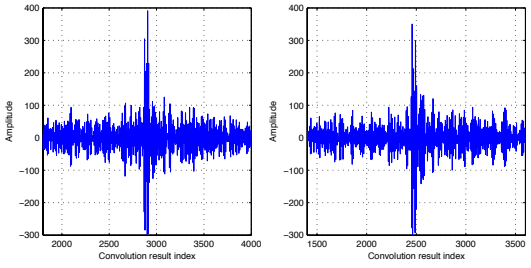

Fig. 5. Matched filter convolution - Indirect path detection

As it can be seen from Fig. 5, the output of the matched filter from the two selected trials has two very close distinct maximums, evidencing the presence of a strong secondary path that strongly affects precision of the system based on the adopted the decision criteria so far. After a detailed analysis of the convolution results of the four channels for all detections it was concluded that Fig. 5 is quite representative of what happened throughout the test. In Fig. 6 it is presented an histogram of the time difference between the two convolution maximums for the different channels.

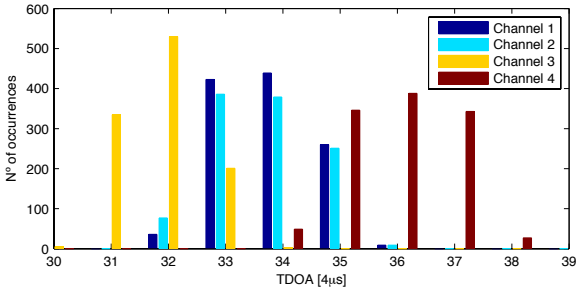

Fig. 6. Histogram of the time difference between the two convolution maximums

As it is clearly shown in Fig. 6 the time difference between the two convolution maximums varies from channel to channel. That difference is greater for channel 4 convolutions, smaller for channel 3 and intermediate for channels 1 and 2. Taking into account the above remarks and knowing that channel 4 is connected to the the deepest hydrophone, channel 3 to the hydrophone closest to the surface and channels 1 and 2 to the hydrophones at intermediate depth, it is coherent to suspect that that the second maximum in the matched filter output was caused by a signal reflection on the sea surface, whereas the first maximum was caused by a direct path signal arrival.

In order to tackle this multi-path detection problem, and based on the experimental evidence, a new TOA estimation method was adopted: when the decision criteria given by (3) is true, instead of estimating the TOA as the absolute maximum the TOA is considered to be be given by the first maximum that exceeds the decision threshold. In Fig. 7 the histogram results from Fig. 4 are reproduced, obtained by post-processing the data acquired during the test with the new TOA estimation method.

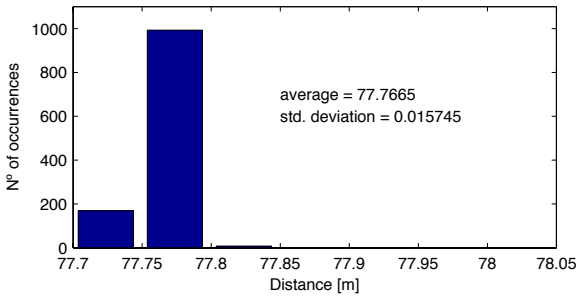

Fig. 7. Histogram of stationary test distance results with new TOA estimation method

As it can be seen from Fig. 7, with the new TOA estimation method, the measured distances are no longer divided between two non-contiguous sub-intervals and the standard deviation is reduced form 8.8cm to 1.6cm. This new TOA estimation method yields better multi-path rejection and therefore global system performance is greatly improved.

The effects of multi-path poor performance rejection affected more severely the on line computation of the emitter's direction. The inconsistent direction results are justified also by inconsistent TDOA estimation. As previously reported in distance computation (Fig. 4), TDOA results are also divided between non-contiguous sub-intervals. The time difference between those sub-intervals, 30 to 40 samples, is similar (see Fig. 6) suggesting that the problem may be caused by signal reflection as before. Thus, to avoid multi-path detection related discrepancies, the new TOA estimation method was also applied for post-processing of the direction computation. As expected, the new TOA estimation method greatly improves TDOA estimation, yielding a TDOA precision of about $8\mu s$ (2 samples). The post-processed direction computation results using the new TOA and TDOA estimation methods revealed a performance enhancement, with a standard deviation of 0.4 deg.

Time delay estimation techniques can be found in the literature, resorting to a method based on the cross-correlation of the acoustic data between the different channels. With the purpose of computing the signal TDOA to the different hydrophones, the cross-correlation method was also employed in post-processing analysis. Due to the lack of space, the results obtained are not presented here but they revealed an interesting feature: cross-correlation performance depends on the channels being processed, for the particular experimental setup used in this work. Similar performance was achieved for the TDOA estimation between channels 1 and 2, which are connected to hydrophones at the same depth, and inferior performance for any other two channels. This result is also justified by signal reflection and hydrophone placement at different depths.

4.2 *Dynamic tests*

For the dynamic tests the emitter was installed in a small rubber boat with GPS position logging capabilities. The distance and angles intervals that was possible to test were very limited. Still, the dynamic test was conducted inside the harbor to allow adequate fastening of the USBL receiving array, and with a duration of 1445 s (approximately 24 min). Since the DSSS signal was being emitted once per second there would be 1445 possible detections. However, 203 emissions were lost (14% of total) and the computed distance results for the dynamic test is shown in Fig. 8 distance (lost emissions are plotted at 0 m distance).

In addition to the lost emissions there were detections that clearly lead to incorrect distance results. These incorrect results were caused by direct path signal poor detection and correspondent multi-path detection. In order to quantify these cases a maximum speed of 4m.s^{-1} was considered for the emitter and a particular distance result is classified as incorrect if it is incoherent with the considered maximum speed and the

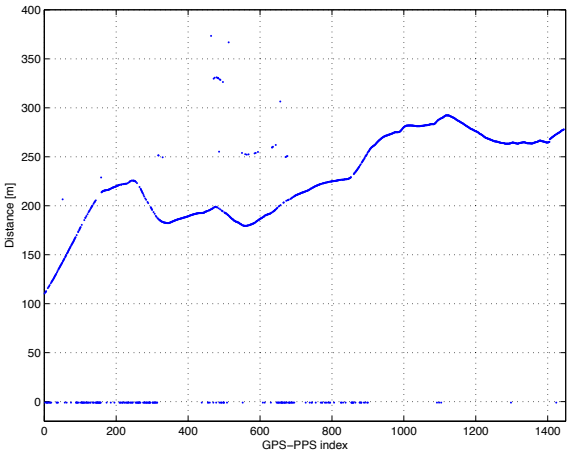

Fig. 8. Dynamic test distance results relative to initial experiment time

previous detection. Using this classification scheme 1210 from the previous 1242 detections were in fact classified as correct (84% of 1445 total emissions).

To assess the system performance computing the emitter's direction the same classification analysis strategy was adopted. The direction results are not plotted but percentage of coherent results is presented in Table 1. The direction performance comparison was obtained with two different methods for TDOA estimation previously mentioned: the first, by selecting the first convolution maximum that exceeds the decision threshold, and the latter data cross-correlation between channels. For this analysis only the 1210 receptions that were classified as coherent distance results were used.

Table 1. Dynamic test direction results

	θ	ϕ
Matched filter peak	822 (68%)	866 (72%)
Cross-correlation	986 (81%)	1007 (83%)

Unlike the results obtained for the stationary test, the cross-correlation method revealed a slightly improved performance in the dynamic test setup. Moreover, the performance was found to be very similar between the longitudinal and elevation angles. However, as evidenced during the stationary tests, the cross-correlation method performance depended on the channels being processed and the performance was considerably better for the TDOA estimation of the channels connected to hydrophones at the same depth and therefore sufficient to compute the longitudinal angle. Even though computing the direction of the emitter using all 4 hydrophones provides some redundancy, a further post-processing analysis was conducted bypassing the least squares minimization presented in Section 2, and computing the longitudinal angle using channels 1 and 2 (same depth) and channels 3 and 4 (different depths) for the elevation angle.

The results presented in Table 2 show the performance improvement using the cross-correlation method, being that the performance between longitudinal and elevation angles is now quite different. Longitudinal

Table 2. Dynamic test direction results without least squares minimization

	θ	ϕ
Matched filter peak	1121 (93%)	902 (75%)
Cross-correlation	1203 (99%)	1008 (83%)

angle performance significantly improves, approaching 100% of correct results, while the elevation angle performance remains at the same level. This decoupling analysis show that the least square minimization was affecting the expected system performance for the particular experimental setup. Nevertheless, least square minimization should be a good option when the TDOA estimation error is similar between channels.

The global attainable performance and the future potential of the system being developed is assessed by comparing the estimated position of the emitter using the USBL device with the emitter GPS tracking. In Fig. 9 the emitter's GPS measured positions are compared with the USBL computed positions from the coherent distance and longitudinal angle results obtained without least squares minimization.

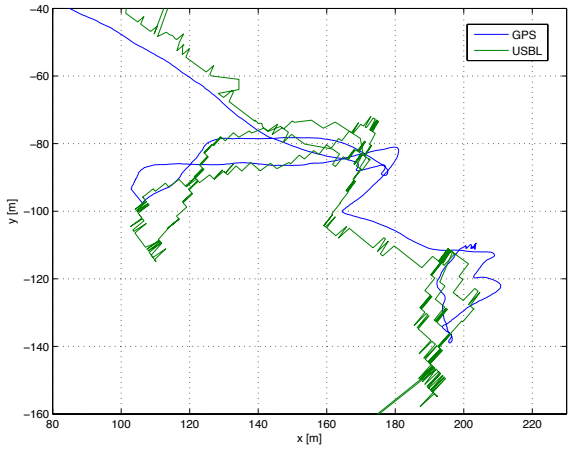

Fig. 9. GPS vs. USBL positioning

5. CONCLUSIONS

This paper presented the design, implementation, and validation at sea of an USBL acoustic positioning system. Signal detection and TOA estimation were based on the matched filters of DSSS coded signals which allows improved detection in a variety of SNR scenarios, and stronger multi-path rejection. Experimental validation tests were conducted inside an harbor, using both static and moving scenarios. Throughout the tests, signal surface reflections were found to highly affect the overall performance of the proposed positioning system. Several TOA estimation techniques were tested by post-processing the acquired data revealing excellent multi-path rejection rates and improved accuracy. Future work will focus on the further development and calibration of the prototype system and the acoustic signaling techniques to allow for a feasible and implementable underwater positioning system.

6. REFERENCES

Austin, T.C. (1994). The application of spread spectrum signaling techniques to underwater acoustic navigation. In: *Proceedings of the 1994 Symposium on Autonomous Underwater Vehicle Technology, 1994. AUV '94*.

Bingham, B., B. Blair and D. Mindell (2007). On the design of direct sequence spread-spectrum signaling for range estimation. In: *OCEANS 2007*. pp. 1–7.

Bingham, B., D. Mindell and T. Wilcox (2005). Integrating sharps ii precision navigation into jason/medea two-vehicle operation. In: *OCEANS, 2005. Proceedings of MTS/IEEE*. pp. 1603–1609 Vol. 2.

Larsen, M.B. (2000). Synthetic long baseline navigation of underwater vehicles. In: *Proceedings of the MTS/IEEE TECHNO-OCEAN Oceans'04 Conference*. Vol. 3. Providence, RI, USA. pp. 2043–2050.

Lee, P.M., B.H. Jeon, S.M. Kim, H.T. Choi, C.M. Lee, T. Aoki and T. Hyakudome (2004). An integrated navigation system for autonomous underwater vehicles with two range sonars, inertial sensors and Doppler velocity log. In: *Proceedings of the MTS/IEEE TECHNO-OCEAN Oceans'04 Conference*. Vol. 3. Kobe, Japan. pp. 1586–1593.

Lurton, X. and N.W. Millard (1994). The feasibility of a very-long baseline acoustic positioning system for AUVs. In: *Proceedings of the IEEE OCEANS '94 Conference*. Vol. 3. Brest, France. pp. 403–408.

Milne, P.H. (1983). *Underwater Acoustic Positioning Systems*. Gulf Pub. Co.

Morgado, M., P. Oliveira, C. Silvestre and J.F. Vasconcelos (2006). USBL/INS Tightly-Coupled Integration Technique for Underwater Vehicles. In: *Proceedings Of The 9th International Conference on Information Fusion*. IEEE. Florence, Italy.

Sarwate, D. V. and M. B. Pursley (1980). Crosscorrelation properties of pseudorandom and related sequences. *Proceedings of the IEEE* **68**(5), 593–619.

Smith, S.M. and D. Kronen (1997). Experimental results of an inexpensive short baseline acoustic positioning system for AUV navigation. In: *Proceedings of the MTS/IEEE Oceans'97 Conference*. Vol. 1. Halifax, Nova Scotia, Canada. pp. 714–720.

Vickery, K. (1998). Acoustic positioning systems. New concepts - The future. In: *Proceedings Of The 1998 Workshop on Autonomous Underwater Vehicles, AUV'98*. Cambridge, MA, USA.

Yli-Hietanen, J., K. Kalliojarvi and J. Astola (1996). Low-Complexity Angle of Arrival Estimation of Wideband Signals Using Small Arrays. In: *Proceedings 8th IEEE Signal Processing Workshop on Statistical Signal and Array Processing*.